Goal-oriented scheme for taming chaos with a weak periodic perturbation: Experiment in a diode resonator

Hong-Jyh Li and Jyh-Long Chern*
Department of Physics, National Sun Yat-sen University, Kaohsiung, Taiwan 80424, Republic of China
(Received 20 June 1995; revised manuscript received 24 April 1996)

We employed the concept of Shannon entropy to characterize the periodicity of the output wave form of a modulated nonlinear diode resonator. A goal-oriented scheme for taming chaos with a weak periodic perturbation is experimentally demonstrated. It is found that a resonancelike regularity is exhibited when the perturbation frequency f_w follows $f_w = f_m/n$, where f_m is the modulation frequency and n is an integer. When f_w is roughly equal to f_m/n and n is small, there exists a low-period orbit, while a larger n results in a high-period orbit. The perturbation's intensity can change the periodicity dramatically; however, as f_w is chosen to be f_m/n^*, the smallest periodicity of the output wave form is n^*. This regularity disappears as n becomes too large ($\sim$1000) and other dynamics takes place. [S1063-651X(96)04808-8]

PACS number(s): 05.45.+b

In the past few years there has been a lot of theoretical and experimental works exploring the field of controlling chaos. Practical implementation of mastering chaos has been of great interest and importance [1]. One of the advantages of controlling chaos is that a variety of unstable periodic orbits embedded in a chaotic attractor can be stabilized [2]. Since the desired periodic orbit can be stabilized, this means that chaos can be utilized for the use of a novel functional generator without greatly modifying the system. This has been emphasized by Ott, Grebogi, and Yorke (OGY) and their OGY method has been a classical means in the field of controlling chaos [2]. However, in response to the dynamics of a high-speed system the OGY method requires a fast enough feedback mechanism that may be impractical for implementation. This difficulty actually occurs to almost all control schemes that are based on feedback or a closed-loop configuration. On the other hand, Braiman and Goldhirsch (BG) theoretically illustrate a nonfeedback (open-loop) scheme [3] for creating periodic orbits as an alternative way of controlling chaos [4]. It is shown that taming chaos can be achieved simply by introducing a suitable weak periodic perturbation to the system. The method proposed by BG is attractive because its implementation in real experiments, particularly high-speed systems, is simple. Strictly speaking, the BG scheme is not a control scheme. As indicated in Ref. [1], there exists a serious weakness in the BG method; i.e., the output is unpredictable. *Is it possible to remove this weakness? Is it possible to develop a goal-oriented scheme for taming chaos with a weak periodic perturbation*? We recently have shown theoretically such a possibility [5]. In this paper, we will experimentally demonstrate the proposed scheme in a nonlinear diode resonator.

First, we should briefly summarize our previous work [5]. Essentially, we treat a time series as a symbol sequence from an information source. Suppose that we have such an information source S, which can generate a set of different symbols $\{s_1,s_2,s_3,\ldots,s_q\}$ with the probability of occurrence $\{P(s_1),P(s_2),P(s_3),\ldots,P(s_q)\}$. The Shannon entropy $H(S)$ follows $H(S)=-\sum_{j=1}^{q} P_j \log_2 P_j$. As an example, referring to the boxes shown in Fig. 1, there are two different types of period-3 attractors. They are noted as B_u for the upper box and B_d for the lower one. If we take the maxima as the information events, the sources B_u and B_d emit the sequences $\{a_1,b_1,c_1,\ldots\}$ where $a_1 \neq b_1 \neq c_1$ and $\{a_2,b_2,c_2,\ldots\}$ where $a_2=b_2\neq c_2$, respectively. Thus, for B_u, $P(a_1)=P(b_1)=P(c_1)=1/3$ and $H(B_u)=1.585$. For B_d, $P(a_2)=2/3(a_2=b_2)$, $P(c_2)=1/3$, and $H(B_d)=0.918$. Therefore, we can distinguish these two different attractors by the value of the Shannon entropy. However, by this way

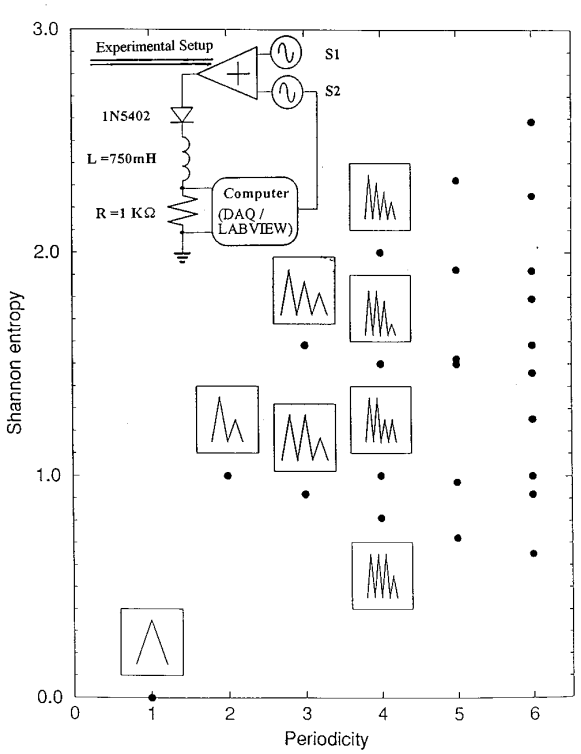

FIG. 1. The values of Shannon entropy at different periodicity. A wave form within one circle is shown in the box for illustration (see text). The experimental setup is shown in the upper portion where $S1$ means the main signal source; $S2$: the weak signal source controlled by the LabVIEW through a GPIB interface; DAQ: data acquisition board.

*Address after August 1996: Department of Physics, National Cheng Kung University, Tainan 701, Taiwan, Republic of China.

 © 1996 The American Physical Society

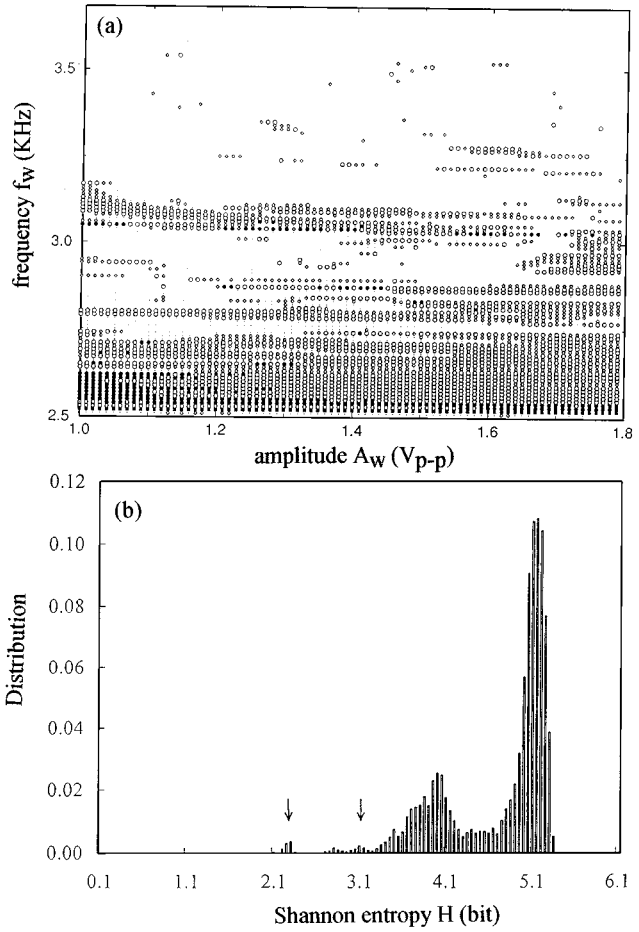

FIG. 2. (a) A two-dimensional diagram of entropy distribution. The x axis and y axis show the amplitude and frequency of applied weak perturbation. The solid square is for $2.0 \leqslant H < 2.5$ where H is the Shannon entropy. The empty square, solid circle, and empty circle are for $2.5 \leqslant H < 3.0$, $3.0 \leqslant H < 3.5$, and $3.5 \leqslant H < 4.0$, respectively. The diamond shows $4.0 \leqslant H < 4.5$ and the dotted point indicates $4.5 \leqslant H < 5.0$. For $H \geqslant 5.0$, no label has been made. (b) The histogram of the perturbed states in terms of entropy value.

of calculation, a one-to-one correspondence between the periodicity and the Shannon entropy is lost. We cannot precisely identify the periodicity. Nevertheless, we always can remove this ambiguity by defining a different kind of Shannon entropy. Practically, the use of the Shannon entropy of-

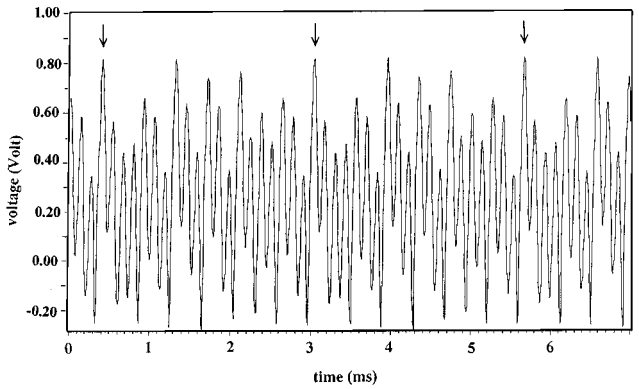

FIG. 3. Time series of a tamed period-20 orbit. The parameters are $f_m = 7.6$ kHz, $A_m = 20.0$ $V_{p\text{-}p}$, $f_w = 3.199$ kHz, and $A_w = 1.72$ $V_{p\text{-}p}$.

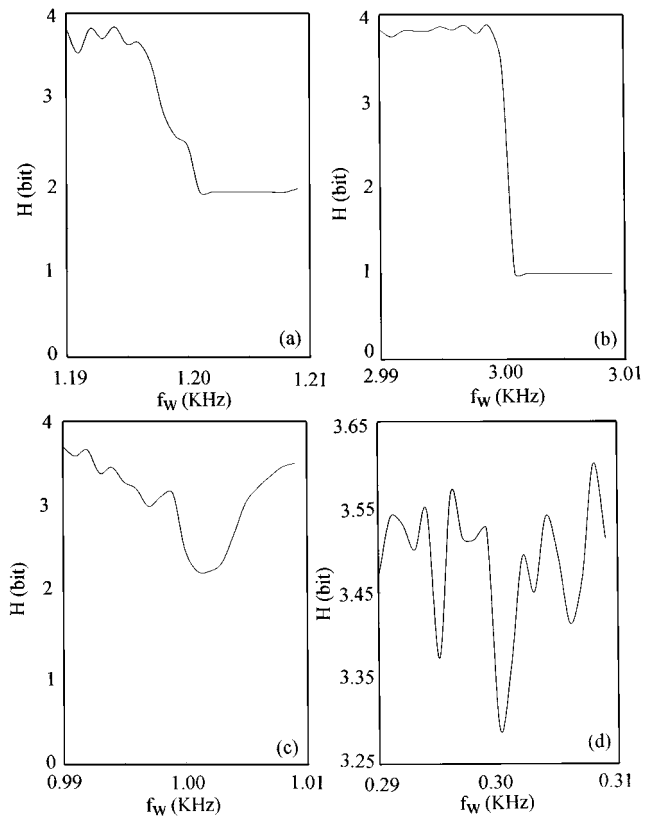

FIG. 4. Variation of entropy value with perturbation frequency where $f_m = 6.0$ kHz and $A_m = 20.0$ $V_{p\text{-}p}$. (a) $n = 5$ with $A_w = 0.7$ $V_{p\text{-}p}$; (b) $n = 2$ with $A_w = 1.3$ $V_{p\text{-}p}$; (c) $n = 6$ with $A_w = 1.83$ $V_{p\text{-}p}$; and (d) $n = 20$ with $A_w = 1.72$ $V_{p\text{-}p}$.

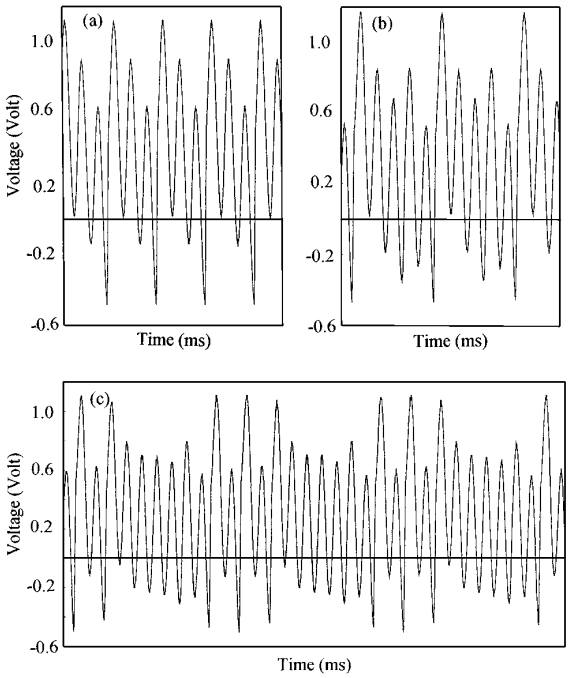

FIG. 5. Regular time series appear near the resonancelike regions. (a) $n = 3$ and $A_w = 1.53$ $V_{p\text{-}p}$; (b) $n = 5$ and $A_w = 0.73$ $V_{p\text{-}p}$; and (c) $n = 11$ and $A_w = 1.5$ $V_{p\text{-}p}$.

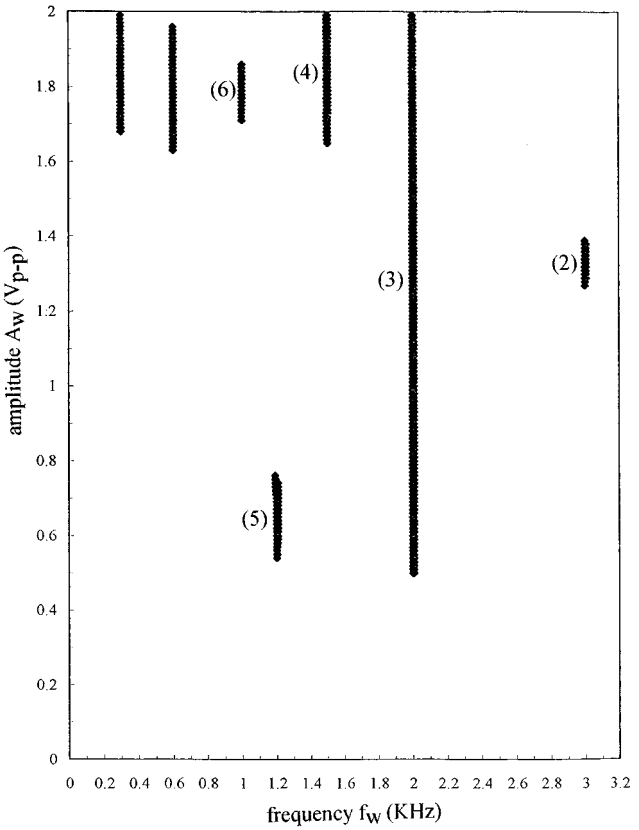

FIG. 6. The distribution region of output wave form with smallest periodicity in terms of f_w and A_w where $f_m = 6.0$ kHz and $A_m = 20.0$ $V_{p\text{-}p}$. The number in parentheses is the corresponding periodicity directly identified by time series.

fers a convenient and efficient way to monitor the periodicity of the attractor as shown below.

Next, we summarize our searching procedure. In step 1, we take the data of the time series, say $X(t)$, with some starting parameter value and pick up N successive maxima of $X(t)$, i.e., $\{X_i\}$ $(i=1,2,3,\ldots,N)$. In step 2, we classify these X_i according to their values, and then count the number of X_i appearing in each group. We label them as N_j where $j=1,2,3,\ldots,M$ and M is the number of groups being classified. After this, by dividing N_j with N, we determine the probability P_j and calculate the Shannon entropy H, which is defined above. In step 3, we switch to the next parameter and return to step 1 to search the region of a lower entropy value. In our experiment, the complexity of a wave form is indicated by measuring the entropy. We can lead the system away from chaos by adopting some condition statements in a searching program. Practically, we first take four trials to determine the entropy in the nearby region of the initial parameters and drive the system to the region of the lowest entropy. By repeating this procedure we gradually direct the system toward the desired periodic region. Since it is the periodic region that we are searching, we do not need to accumulate a large amount of data in calculating the entropy. We should note that the Shannon entropy determined here is resolution dependent. If the resolution is low, we may mistake a high-period attractor for a lower-period attractor. That becomes a problem especially when we want to use the Shannon entropy to identify high periodicity or when the noise exists. Generally, we should choose the highest resolution that we possibly can.

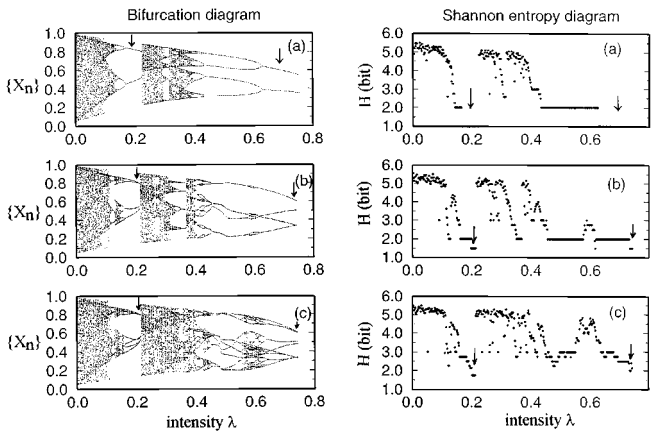

FIG. 7. Bifurcation diagram and Shannon entropy diagram for a modified logistic mapping. (a) Driven by a period-2 orbit; (b) driven by a period-4 orbit; and (c) driven by a period-8 orbit. We use λ to represent the perturbation intensity.

In the following, we first report our experimental setup. Referring to Fig. 1, the resonator circuit consists of a silicon rectifier in series with an inductor. We use the diode 1N5402 and a 750-mH inductor with 1-kΩ dc resistor. This system exhibits a classical period-doubling sequence as it is driven with a sinusoidal voltage [6]. We denote the driven frequency and amplitude as f_m and A_m. An additional driving signal will be used as a weak perturbation. For this weak periodic perturbation, we label the frequency and amplitude as f_w and A_w. For automatic searching, we run our experiment with the software NI LabVIEW. The time series of the voltage across the resistor is sampled by a data acquisition board and the peak voltages (and the entropy) are determined by programming with NI LabVIEW. The number of sampled peaks is 700 here. We adopted the resolution 0.02 V here. In the course of the experiment, we always keep the highest sampling rate of 200 kHz.

Next, we report the experimental result. We set $f_m = 7.6$ kHz and $A_m = 20.0$ $V_{p\text{-}p}$ (p-p denotes peak to peak; i.e., the wave form oscillates between 10 and -10 V). With this condition, chaos appears. We further apply a weak perturbation to the circuit. By varying the weak signal, we derive a phase diagram as shown in Fig. 2(a), which contains 9600 perturbed states. One can see that various wave forms have been generated. To explore the feature quantitatively, we count each perturbed state according to the entropy. After dividing with the total number of perturbed states, we derive a histogram. As shown in Fig. 2(b), a high value in distribution promises a high probability of finding correspondent periodic orbit. If we start our searching randomly, we can estimate the searching efficiency based on such a distribution. As indicated by the down arrows in Fig. 2(b), low-period orbits can be created whereas the high-period orbits, corresponding to high entropy value, can also be excited. A typical example of a period-20 orbit is shown in Fig. 3 in which the period is indicated by two successive down arrows. This contradicts the previously recognized idea that high-period orbits are impossible to create by making only one correction in the long period because of the inherent nature of chaos [7]. These results show that to create and

search the desired periodic orbits is rather promising provided that there is a suitable distribution.

It is worthwhile to note that there appears a large portion of periodic region near $f_w = 2.53$ kHz that is very close to $f_m/3$. (Note that $f_m = 7.6$ kHz.) It implies that some regularity may occur when $f_w = f_m/n$, where n is a certain integer, such as 2,3,4, ... Qualitatively, it seems that the system exhibits a resonancelike feature [8], which can be well characterized by the drop of Shannon entropy as shown below. The variation of the Shannon entropy shown in Fig. 2(a) suggests that the periodicity of the output wave form depends not only on the frequency of weak perturbation but also on the amplitude. Actually, some nontrivial features can be revealed by exploring the resonancelike region, particularly with the help of the Shannon entropy characterization. For an illustration, we take $f_m = 6.0$ kHz and $A_m = 20.0$ $V_{p\text{-}p}$ and vary the f_w and A_w. As shown in Fig. 4(a), a drop of the Shannon entropy appears at $f_w = f_m/5$. In Fig. 4(b), a similar feature is exhibited for a lower n as $f_w = f_m/2$. Again, in Fig. 4(c), a deeper drop appears near $f_w = f_m/6$. Higher n also appears just as commonly. As shown in Fig. 4(d), a deeper drop of the Shannon entropy occurs to the region near $f_w = f_m/20$. On can clearly see that a high Shannon entropy value is associated with the region with high n. This suggests that by using a larger n for $f_w = f_m/n$, one can create a high-period orbit. We verify this statement by a direct investigation of time series. As shown in Fig. 5(a), an output wave form with periodicity $p = 3$ occurs for $f_w/f_m = 0.334$. Here $f_m/f_w = n = 3$. Another example is $p = 5$, which is exhibited in the system as $f_w/f_m = 0.2$. Here $f_m/f_w = n = 5$. It will be very useful to show a higher p. We show an output wave form with periodicity $p = 11$, which occurs when $f_w/f_m = 0.091$. Here $n = 11$. However, as n becomes too large (~ 1000), i.e., f_w becomes only a few Hz, a completely different dynamics takes place. Specifically, there appears a circulation among different (unstable) attractors. This is similar to the ''breathing effect'' reported by Qu *et al.* [9]. Since we are unable to provide a clever characterization beyond the work of Qu *et al.* [9], we will not address it here. Roughly, we can conclude that for a certain f_m, by using a weak perturbation with a frequency $f_w = f_m/n$, where n is almost an arbitrary integer, one can generate some regular wave form provided that the amplitude is suitable. Since the amplitude A_w can change the periodicity p dramatically, we are led to consider the following question. *What is the smallest periodicity one can obtain for the output wave form when n is equal to a specified value, say n*, and* $f_w = f_m/n^*$? For investigation, we vary the perturbation's intensity. It seems to us that the smallest periodicity is n^*. We present a part of the evidence in Fig. 6.

For comparison, we also adopt some other theoretical models [5] for investigation. Here, for simplicity, we present our result of the modified logistic mapping. The equations are

$$X_{n+1} = r_1 X_n (1 - X_n) - \lambda Y_n , \tag{1}$$

$$Y_{n+1} = r_2 Y_n (1 - Y_n). \tag{2}$$

We set $r_1 = 3.9$. As $\lambda = 0$, chaos appears for $\{X_n\}$. We change r_2 to generate the time series of Y_n with a specific periodicity p, say $p = 2$ or 4. After transient, we use only 50 X_n to make the bifurcation diagram and 100 X_n for the Shannon entropy diagram. One can see that the chaos is suppressed and transformed into various dynamic states for different λ. Let us look at Fig. 7(a) where the periodicity of $\{Y_n\}$ is 2. As indicated by the down arrow, one can see that the smallest periodicity of the output wave form, i.e., $\{X_n\}$, is 2. This is exactly the same as the periodicity of Y_n. This feature also can be seen, e.g., when the periodicity of $\{Y_n\}$ is 3. It should be noted that there are some empty regions in the diagrams of Fig. 7. These appear simply because X_n is out of the range of [0,1]. We have checked the periodicity of Y_n up to 16. Unfortunately, to clarify the general features, there remains much work to be done.

In conclusion, we have demonstrated the experimental feasibility of the proposed scheme described in Ref. [5]. This work shows the robustness of the proposed scheme in a real system. It should be remarked that by using different types of weak perturbations, such as square, triangle, and ramp wave forms, and different chaotic states as the target of perturbation, we have derived a series of bifurcation diagrams and histograms. It seems safe to conclude that a weak periodic perturbation usually results in high-period orbits or even chaos. Low-period orbits occur in the resonancelike regions provided that the frequency of weak perturbation follows $f_w = f_m/n$, where n is small and the amplitude A_w is suitable. However, n could not be too large. We found that as f_w is around a few Hz where f_m is around a few kHz, the system displays a circulation feature, i.e., different (unstable) attractors that can be identified rather clearly appear successively and repeatedly. Nevertheless, it is possible to excite the high-period orbit with high n as shown above.

This work was partially supported by the National Science Council, R.O.C. under Contract No. NSC 84-2112-M110-004.

[1] T. Shinbrot *et al.*, Nature **363**, 411 (1993).
[2] E. Ott *et al.*, Phys. Rev. Lett. **64**, 1196 (1990).
[3] Y. Braiman and I. Goldhirsch, Phys. Rev. Lett. **66**, 2545 (1991).
[4] A. Hubler and E. Luscher, Naturwissenschaften **76**, 365 (1989).
[5] H. J. Li and J. L. Chern, Phys. Rev. E **52**, 297 (1995).
[6] P. S. Linsay, Phys. Rev. Lett. **47**, 1349 (1981); J. Testa, *et al.*, *ibid*. **48**, 714 (1982); R. W. Rollins and E. R. Hunt, *ibid*. **49**, 1295 (1982).
[7] E. R. Hunt, Phys. Rev. Lett. **67**, 1953 (1991).
[8] R. Lima and M. Pitti, Phys. Rev. A **41**, 726 (1990); A. Y. Loskutov and A. I. Shishmarev, Chaos **4**, 391 (1994); S. T. Vohra, *et al.*, Phys. Rev. Lett. **75**, 65 (1995).
[9] Z. Qu, *et al.*, Phys. Rev. Lett. **74**, 1736 (1995).